crystals

MDPI

Article

Symmetry-Adapted Finite Strain Landau Theory Applied to $KMnF_3$

Andreas Tröster [1,*], Wilfried Schranz [1], Sohaib Ehsan [2], Kamal Belbase [2] and Peter Blaha [2]

[1] Faculty of Physics, University of Vienna, Boltzmanngasse 5, A-1090 Vienna, Austria; wilfried.schranz@univie.ac.at
[2] Institute of Materials Chemistry, Vienna University of Technology, Getreidemarkt 9, A-1060 Wien, Austria; sohaib.ehsan@tuwien.ac.at (S.E.); kamal.belbase@tuwien.ac.at (K.B.); peter.blaha@tuwien.ac.at (P.B.)
* Correspondence: andreas.troester@univie.ac.at

Received: 27 January 2020; Accepted: 11 February 2020; Published: 17 February 2020

Abstract: In recent years, finite strain Landau theory has been gradually developed as both a conceptual as well as a quantitative framework to study high pressure phase transitions of the group-subgroup type. In the current paper, we introduce a new version of this approach which is based on symmetry-adapted finite strains. This results in a substantial simplification of the original formulation. Moreover, it allows for replacing the clumsy use of truncated Taylor expansions by a convenient functional parametrization. Both the weaknesses of the traditional Landau approach based on infinitesimal strains as well as the major improvements made possible by our new parametrization are illustrated in great detail in an application to the ambient temperature high pressure transition of the perovskite $KMnF_3$.

Keywords: high pressure; phase transitions; Landau theory; nonlinear elasticity theory; perovskites

1. Introduction

Through many decades, the Landau theory (LT) of phase transitions [1,2] (PTs) has proven to be one of the most valuable conceptual tools for understanding PTs of the group-subgroup type. In particular, the field of structural PTs abounds even with successful quantitative applications, and, for many classes of materials, complete collections of the corresponding coupling coefficients have been gathered in the literature (for ferroelectrics see, e.g., Appendix A of Ref. [3]). Effects of spontaneous strain that generally accompany temperature-driven structural PTs are sufficiently parameterized in terms of infinitesimal strain tensor components defined with respect to a baseline, which is obtained by extrapolating the generally small thermal expansion changes of the high symmetry reference phase. The corresponding Landau potential then involves only terms up to harmonic order, and any temperature dependence of the relevant parameters (high symmetry phase elastic constants and other coupling constants) can usually be completely neglected [4].

The situation changes drastically for high pressure phase transitions (HPPTs). Spontaneous strain components may still be numerically small, but they now must be defined with respect to a P-dependent base line. The total strain measured with respect to the ambient pressure reference state must then be calculated from a nonlinear superposition of finite background and spontaneous strain (see Equation (11) below). Furthermore, the Landau potential may be truncated beyond harmonic order only if calculated with respect to this P-dependent elastic background reference system. Therefore, neither the elastic constants nor the other elastic couplings can be assumed to be P-independent. In a high pressure

context, clinging to the familiar infinitesimal strain Landau toolbox may result not only in a quantitatively, but also qualitatively completely erroneous description.

It is not easy to construct a mathematically consistent and yet practically useful version of Landau theory taking into account the inherent nonlinearities and anharmonic effects that accompany HPPTs. In recent years, however, such a theory, for which we have coined the name finite strain Landau theory (FSLT), has been successfully developed. FSLT constitutes a careful extension of Landau theory beyond coupling to infinitesimal strain, fully taking into account the nonlinear elastic effects at finite strain. Its capabilities have been demonstrated in a number of applications to HPPTs [5–10]. However, as it stands, the numerical scheme underlying FSLT is still quite involved, and many practical workers in the field of HPPTs may be hesitant to go through the mathematical hardships it seems to pose. It is the purpose of this paper to show that FSLT is drastically simplified by switching from a formulation in terms of Cartesian Lagrangian strains to one in terms of symmetry-adapted finite strains. The enormous reduction of overall complexity of the approach as well as the vastly reduced numerical requirements of our new version of FSLT are demonstrated on the example of the HPPT in the perovskite $KMnF_3$ (KMF).

2. Review of Experimental Results on the Cubic-to-Tetragonal Transition of KMF

In what follows, we focus on the antiferrodistortive high pressure phase transition of KMF from the cubic perovskite aristophase $Pm\bar{3}m$ to a tetragonal $I4/mcm$ phase at room temperature which was experimentally investigated in Ref. [11] by X-ray diffraction up to 30 GPa. Since the ambient pressure Landau theory also provides a limiting reference frame for the description of the high pressure transition, we start our discussion with a detailed survey of the corresponding Landau theory.

According to Ref. [12], a similar transition observed at ambient pressure and temperature $T_c = 186.5$ K is weakly first order but close to critical, and the mechanism underlying these transitions is the same as in the well-studied $T = 105$ K cubic-to-tetragonal transition in strontium titanate, i.e., octahedral tilting with a critical wavevector at the R-point of the cubic Brillouin zone. Furthermore, in Ref. [12], it is argued that, even though a further structural transition to an orthorhombic phase related to further octahedral tilting at the M-point of the Brillouin zone at $T_N = 87$ K is accompanied by antiferromagnetism, this coincidence between structural and magnetic transition temperatures may just be accidental, and actually there seems to be essentially no coupling between structural and magnetic order parameters (OPs) for these transitions. In passing we note that at $T = 82$ K there is a further transition to an orthorhombic canted ferromagnet [12].

As discussed in Ref. [12], the $Pm\bar{3}m \rightarrow I4/mcm$ symmetry reduction corresponds to the isotropy subgroup of the three-dimensional irreducible representation R_4^+ of $Pm\bar{3}m$ with respect to the order parameter direction $(Q,0,0)$, the corresponding Landau expansion to sixth order being

$$\begin{aligned} F \;=\; & \frac{A}{2}\left(Q_1^2+Q_2^2+Q_3^2\right)+\frac{B}{4}\left(Q_1^4+Q_2^4+Q_3^4\right)+\frac{B_2}{4}\left(Q_1^2Q_2^2+Q_2^2Q_3^2+Q_1^2Q_3^2\right) \\ & +\frac{C}{6}\left(Q_1^6+Q_2^6+Q_3^6\right)+\frac{C_2}{6}\left(Q_1^2Q_2^4+Q_2^2Q_3^4+Q_1^2Q_3^4+Q_2^2Q_1^4+Q_3^2Q_2^4+Q_3^2Q_1^4\right)+\frac{C_3}{6}Q_1^2Q_2^2Q_3^2 \\ & +\lambda_a^{(0)}(Q_1^2+Q_2^2+Q_3^2)\epsilon_a+\lambda_t^{(0)}(2Q_1^2-Q_2^2-Q_3^2)\epsilon_t+\frac{K^{(0)}}{2}\epsilon_a^2+\frac{\mu^{(0)}}{2}\epsilon_t^2 \end{aligned} \tag{1}$$

with volume and tetragonal symmetry-adapted strains $e_a = e_{11}+e_{22}+e_{33}$, $e_t = \frac{2e_{33}-e_{11}-e_{22}}{\sqrt{3}}$ and bulk and longitudinal shear modulus related to the bare cubic elastic constants by $K^{(0)} = (C_{11}^{(0)}+C_{12}^{(0)})/3$, $\mu^{(0)} = (C_{11}^{(0)}-C_{12}^{(0)})/2$. Targeting a transition into a single tetragonal domain where $(Q_1,Q_2,Q_3) \equiv (Q,0,0)$ and $\epsilon_{22} = \epsilon_{33}$, we have

$$\begin{aligned} F &= \frac{A}{2}Q^2 + \frac{B}{4}Q^4 + \frac{C}{6}Q^6 + \lambda_a^{(0)}Q^2\epsilon_a + 2\lambda_t^{(0)}Q^2\epsilon_t \\ &\quad + \frac{K^{(0)}}{2}\epsilon_a^2 + \frac{\mu^{(0)}}{2}\epsilon_t^2 \end{aligned} \tag{2}$$

In a standard Landau approach, the coefficients $B, C, \lambda_a^{(0)}, \lambda_t^{(0)}$ are assumed to be independent of temperature (and pressure), while for A the ansatz

$$A = A_0(T - T_0) \tag{3}$$

with T-independent coefficients A_0, T_0 is made and quantum saturation has been neglected [13]. The elastic equilibrium conditions $-P = \frac{1}{V_0}\frac{\partial F}{\partial \epsilon_a}\Big|_{\bar{\epsilon}_a,\bar{\epsilon}_t}$ and $0 = \frac{1}{V_0}\frac{\partial F}{\partial \epsilon_t}\Big|_{\bar{\epsilon}_a,\bar{\epsilon}_t}$ amount to

$$\bar{\epsilon}_a = e_a(P) - \frac{\lambda_a^{(0)}}{K^{(0)}}Q^2, \qquad \bar{\epsilon}_t = -\frac{2\lambda_t^{(0)}}{\mu^{(0)}}Q^2 \tag{4}$$

with a background volume strain

$$e_a(P) = 3e(P), \quad e(P) = -\frac{P}{3K^{(0)}} \tag{5}$$

Performing a Legendre transform yields the Gibbs potential

$$G = \frac{A_R}{2}Q^2 + \frac{\widetilde{B}}{4}Q^4 + \frac{C}{6}Q^6 - \frac{P^2}{2K^{(0)}} \tag{6}$$

where

$$A_R = A - 6\lambda_a^{(0)}e(P) = A - \frac{2\lambda_a^{(0)}P}{K^{(0)}} \tag{7a}$$

$$\widetilde{B} = B - \frac{2(\lambda_a^{(0)})^2}{K^{(0)}} - \frac{8(\lambda_t^{(0)})^2}{\mu^{(0)}} \tag{7b}$$

The values of coefficients $A_0 = 63.118\,\mathrm{kPa/K}$, $\widetilde{B} = -1.308\,\mathrm{MPa}$ and $C = 13.032$ MPa at $P = 0$, which imply a first order phase transition at $T_c = 186.15$ K, have been determined from caloric measurements by Salje and coworkers [13]. In principle, numerical values for the OP-strain coupling coefficients $\lambda_a^{(0)}, \lambda_t^{(0)}$ may be extracted from experimental data on the temperature evolution of spontaneous strains $\bar{\epsilon}_a, \bar{\epsilon}_t$. Unfortunately, however, for KMF, this is easier said than done. At room temperature, the thermal expansion data $a_{\mathrm{cubic}}(T)$ of Ref. [14] are observed to perfectly reproduce the value of the cubic lattice constant $a_{\mathrm{cubic}}(T_R)$ at ambient pressure as determined in Ref. [11]. However, the measurement data of thermal lattice parameter irregularities $a(T), c(T)$ around $T_c \approx 186$ K (Refs. [15–18]) available in the literature appear to be in rather poor mutual agreement. As Figure 1 illustrates, while a discontinuous behavior of the lattice parameters is clearly visible in all three data sets, the absolute values of the measured unit cell parameters differ considerably, yet none of the data sets seem to be compatible with extrapolating the thermal expansion data of Ref. [14].

Not unexpectedly, the agreement in relative splitting between the a-and c-axis in the tetragonal phase appears to be better, albeit far from perfect. Nevertheless, the cubic parts of the data of Refs. [15,18] exhibit slopes similar to the low temperature extrapolation of the thermal expansion data of Ref. [14]. In order to be able to collapse the data onto a common "master set", we thus shifted the data of Refs. [15,18] by

constant absolute offsets to match the extrapolated baseline of Ref. [14] in an optimal way, treating the seemingly more precise measurements of Sakashita et al. (Refs. [16,17]) as an outlier. Figure 2 illustrates our results for a corresponding effort.

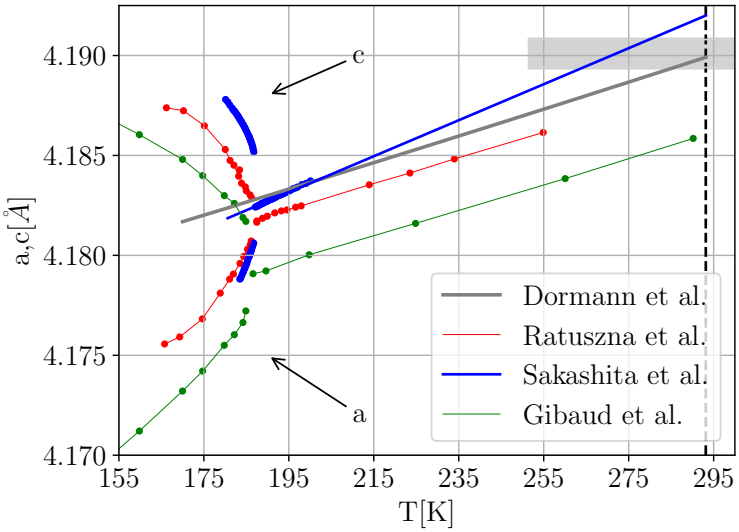

Figure 1. Compilation of experimental unit cell data from Refs. [15] (red) and [18] (green) (data range restricted to $T > 155$ K) [16,17] (blue) and [14] (gray). For comparison, the value (including error bars) of the room temperature (indicated by the vertical dashed line) lattice constant at ambient pressure as measured in Ref. [11] is illustrated by the gray horizontal area.

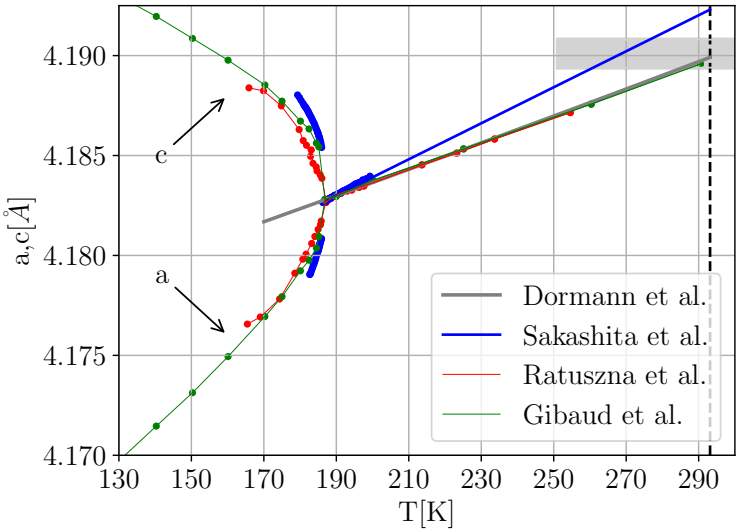

Figure 2. Collapse of data from Refs. [15] (red) and [18] (green), onto the low temperature expansion of the thermal expansion data of Ref. [14] (gray) by constant vertical shifts. The positive and negative branches of the data correspond to values ϵ_t and ϵ_a from the various references, respectively. As in Figure 1, the room temperature ambient pressure lattice constant of Ref. [11] is indicated by a horizontal gray bar for comparison. The shifted data from Ref. [16,17] (blue) clearly appear to be at odds with the other measurements.

With a meaningful baseline $a_{\text{cubic}}(T)$ for unit cell parameters $a(T), c(T)$ in place, we calculate the spontaneous strain components $\epsilon_1 = a/a_{\text{cubic}} - 1$ and $\epsilon_3 = c/a_{\text{cubic}} - 1$ and thus the (infinitesimal) spontaneous volume and tetragonal strains

$$\epsilon_a = 2\epsilon_1 + \epsilon_3 = \frac{2a + c}{a_{cubic}} - 3\,, \tag{8}$$

$$\epsilon_t = \frac{2(\epsilon_3 - \epsilon_1)}{\sqrt{3}} = \frac{2}{\sqrt{3}} \frac{c - a}{a_{cubic}}\,, \tag{9}$$

respectively. According to Equation (4), when plotted against $Q^2(t)$ at $P = 0$, ϵ_a and ϵ_t should resemble straight lines with slopes $-\lambda_a^{(0)}/K^{(0)}$ and $-2\lambda_t^{(0)}/\mu^{(0)}$, respectively. Figure 3 illustrates corresponding fits with results

$$\lambda_a^{(0)}/K^{(0)} = 0.002, \qquad \lambda_t^{(0)}/\mu^{(0)} = -0.005 \tag{10}$$

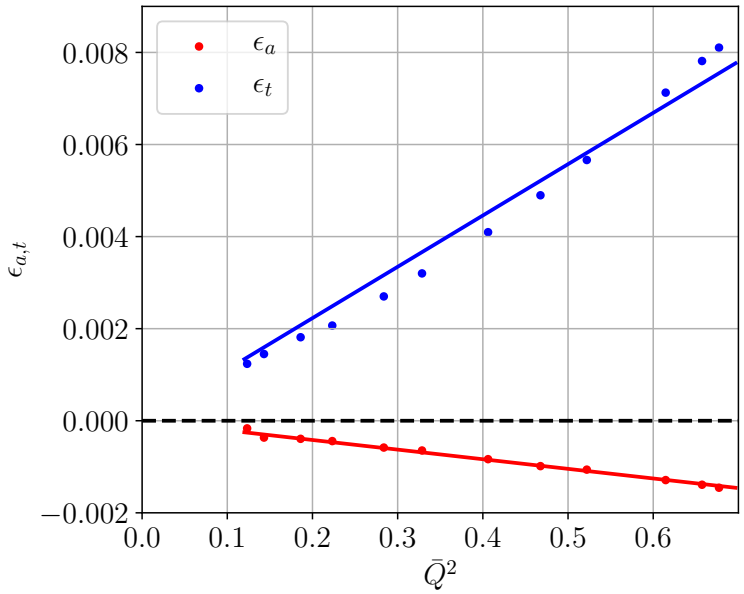

Figure 3. Fits of $\epsilon_a(T)$ and $\epsilon_t(T)$ against $Q^2(T)$ according to Equations (4).

With the Landau theory of the temperature-driven transition at ambient pressure available, we are tempted to analyze the ambient temperature HPPT based on the same framework. In Ref. [11], the variation of the pseudo-/cubic lattice constants of KMF under pressure at room temperature was measured with X-ray scattering (Figure 4) and the cubic part of the data was fitted to a simple Murnaghan equation of state (EOS) with $K_0 = 64\,\text{GPa}$ and $V_0 = 73.608^3$. This provides a baseline to determine (Lagrangian) spontaneous strains $\widehat{\epsilon}_a \approx \epsilon_a, \widehat{\epsilon}_t \approx \epsilon_t$ (Figure 5).

Comparing the thermal and pressure-induced spontaneous strains shown in Figures 2 and 5, respectively, we note that there is some spontaneous thermal volume strain ϵ_a while practically $\widehat{\epsilon}_a \approx 0$ for the pressure-induced case. Furthermore, even though it may be difficult to directly relate temperature and pressure scales, the pressure-induced tetragonal spontaneous strain $\widehat{\epsilon}_t$ is observed to be roughly one order of magnitude larger than its thermal counterpart ϵ_t. From the perspective of traditional Landau theory based on infinitesimal strain coupling, these findings are difficult to explain. Based on Equation (4), there are in principle two ways to alter the magnitude of spontaneous strains. One may either change

the value of the couplings $\lambda_a^{(0)}/K^{(0)}$ and $\lambda_t^{(0)}/\mu^{(0)}$ or find a mechanism to increase the magnitude of $\bar{Q}^2$ which, of course, implicitly depends on all Landau coefficients. Since these are actually only known for $T = 186.5$ K, one could assume a thermal drift in $\lambda^{(0)}$ towards zero to be responsible for the vanishing of $\widehat{\epsilon}_a$ at room temperature (more than counteracting against the thermal drift of K_0 which is generally expected to decrease with increasing T). For the tetragonal strain, a similar mechanism seems to be difficult to conceive, however. On the one hand, we would need to increase $\lambda_t^{(0)}$ dramatically to explain the large values of $\widehat{\epsilon}_t$. On the other hand, Equation (7b) indicates that such an increase would send parameter $\widetilde{B}$ to negative values much larger than those found for the thermal transition, resulting in a pronounced first order character of the HTTP. This, however, is not observed. The only remedy therefore seems to find a way to increase $\bar{Q}^2$. Calculated from a standard 2–4 Landau potential, $\bar{Q}^2$ would be inversely proportional to $1/\widetilde{B}$. This may explain why advocates of an orthodox Landau description frequently resort to assuming HPPT's to be near a tricritical point, explicitly postulating some ad-hoc pressure dependence $\widetilde{B} = \widetilde{B}(P)$ induced somehow by unspecified higher order coupling effects.

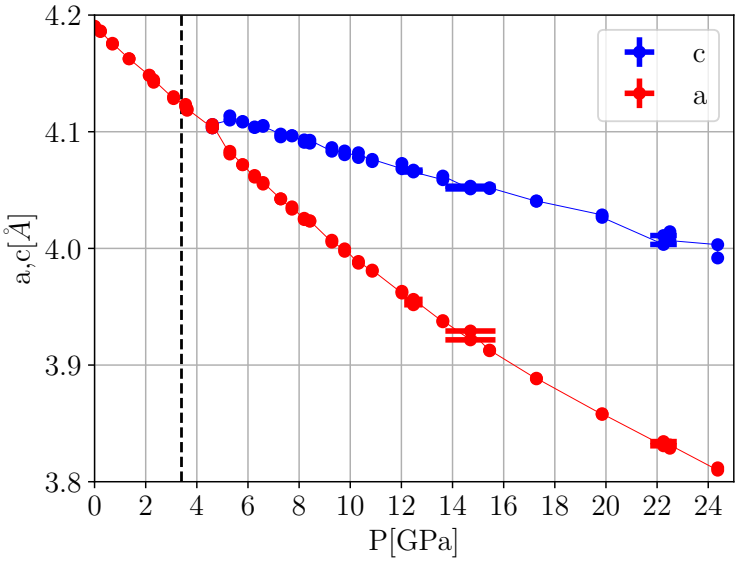

Figure 4. Pseudo-/cubic lattice constants of KMF under pressure at room temperature as measured in Ref. [11] with X-ray scattering. The transition pressure estimate $P_s \approx 3.4$ GPa put forward in Ref. [11], which is indicated by the dashed vertical line, is clearly too low.

Further difficulties arise if we try to reconcile the observed value of P_c with the prediction of standard Landau theory. In Ref. [11], a brute force fit based on the above assumptions of a second order transition close to a tricitical point produced an estimate of $P_c \approx 3.4$ GPa. In principle, for a second order or slightly first order phase transition, this pressure should coincide or be somewhat lower than the pressure value $P_0(T_R)$ at which $A_R(T_R, P_0(T_R))$ vanishes at room temperature T_R. Unfortunately, however, this is incompatible with extrapolating the Landau parametrization of Hayward et al. [19] to room temperature. In fact, inserting the parameter value (10) into Equation (7a) yields $P_0(T_R) \approx 1.7$ GPa, which is completely at odds with $P_c \approx 3.4$ GPa as reported in Ref. [11]. To reach this transition pressure at room temperature would require reducing our previous result $\lambda_a^{(0)}/K^{(0)} = 0.002$ obtained at $T = 186$ K by a full factor of 2 (cf. Figure 6). However, even then, any unbiased reader should have a hard time believing that the bare data of Figure 5 should indicate a continuous transition at $P_c = 3.4$ GPa. In summary, we hope to have demonstrated that standard Landau theory is completely inadequate to describe the HPPT of KMF

unless one is willing to sacrifice any numerical meaning to Landau theory, leaving us with all coupling parameters as essentially unknown and with ad hoc pressure dependencies at room temperature.

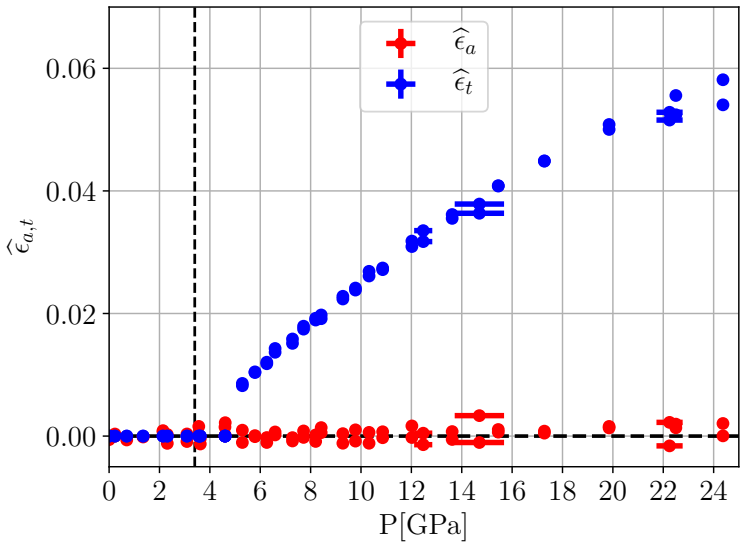

Figure 5. Lagrangian strains $\widehat{\epsilon}_a, \widehat{\epsilon}_t$ calculated from unit cell data and Murnaghan fit of cubic part according to Ref. [11].

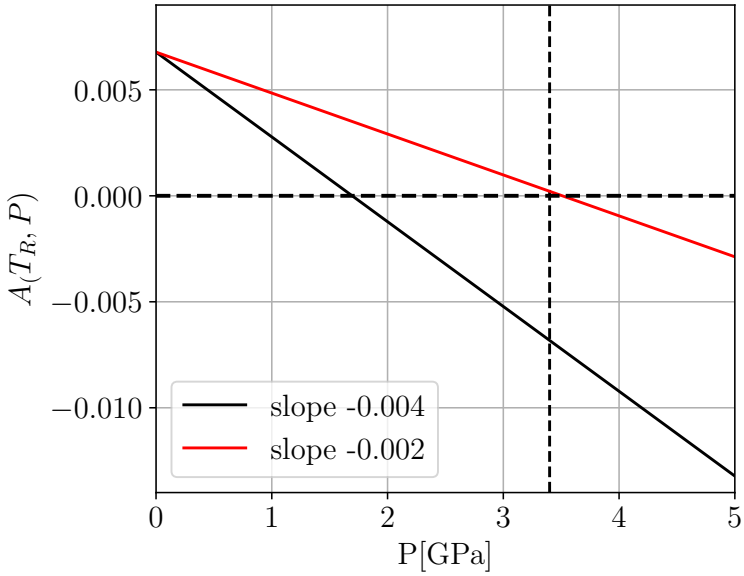

Figure 6. $A_R(T = T_R, P)$ as defined in Equation (10) for correct slope $-2\lambda_a^{(0)}/K^{(0)} = -0.004$ in comparison to a slope of $-2\lambda_a^{(0)}/K^{(0)} \approx -0.002$ assumed in Ref. [11].

3. A Quick Review of FSLT

In a nutshell, in a generic high pressure experiment, a given crystal is observed to change under application of high hydrostatic pressure P from an ambient pressure "laboratory" state $\boldsymbol{X}$ to a deformed state to be denoted as $\widehat{\widehat{\boldsymbol{X}}} = \widehat{\widehat{\boldsymbol{X}}}(P)$ with an accompanying total (Lagrangian) strain η_{ij}. Frequently, a high pressure phase transition manifests itself in such an experiment through the observation of relatively small strain anomalies on top of a much larger "background strain" that in itself is unrelated to the actual transition. Recognizing that the concept of strain is always defined with respect to a chosen elastic

reference state, in Ref. [5], a corresponding background system $\widehat{\boldsymbol{X}} = \widehat{\boldsymbol{X}}(P)$, defined as the (hypothetical) equilibrium state of the system with the primary OP clamped to remain zero, was introduced. Let α_{ik} and $e_{ik} = \frac{1}{2}\left(\sum_n \alpha_{ni}\alpha_{nk} - \delta_{ik}\right)$ denote the deformation and Lagrangian strain tensors from $\boldsymbol{X}$ to $\widehat{\boldsymbol{X}}$, respectively. The total strain η_{ij} may then be disentangled as a nonlinear superposition

$$\eta_{ij} = e_{ij} + \alpha_{ki}\widehat{\epsilon}_{kl}\alpha_{lj} \tag{11}$$

of the—generally large—Lagrangian background strain and a relatively small spontaneous strain $\widehat{\epsilon}_{ij}$ *measured relative to the floating "background" reference state* $\widehat{\boldsymbol{X}}$. Determining the proper background strain e_{ij} in the resulting reference scheme

$$\boldsymbol{X} \xrightarrow{\underline{a},\underline{e}} \widehat{\boldsymbol{X}} \xrightarrow{\underline{\widehat{\alpha}},\underline{\widehat{\epsilon}}} \widehat{\widehat{\boldsymbol{X}}} \qquad \underline{\alpha},\underline{\eta} \tag{12}$$

is thus a crucial step in correctly identifying the actual spontaneous strain, which in turn is mandatory in a successful application of the concepts of Landau theory. Effectively "subtracting" the elastic baseline, the strategy of FSLT therefore consists of setting up Landau theory *within the background reference system* $\widehat{\boldsymbol{X}}$. Based on the reasonable assumption that a harmonic expansion with pressure-dependent elastic constants $C_{ijkl}[\widehat{\boldsymbol{X}}]$ suffices to capture the elastic energy originating exclusively from the relatively small spontaneous strain $\widehat{\epsilon}_{kl}$, one arrives at the Landau free energy

$$\frac{F(Q,\underline{\widehat{\epsilon}};\widehat{\boldsymbol{X}})}{V[\widehat{\boldsymbol{X}}]} = \Phi(Q;\widehat{\boldsymbol{X}}) + \sum_{\mu\geq 1} Q^{2n} d_{ij}^{(2\mu)}[\widehat{\boldsymbol{X}}]\widehat{\epsilon}_{ij} + \frac{F_0(\underline{\widehat{\epsilon}};\widehat{\boldsymbol{X}})}{V[\widehat{\boldsymbol{X}}]} \tag{13}$$

where we have assumed a scalar OP Q for simplicity, and

$$\frac{F_0(\underline{\widehat{\epsilon}};\widehat{\boldsymbol{X}})}{V[\widehat{\boldsymbol{X}}]} \approx \sum_{ij} \tau_{ij}[\widehat{\boldsymbol{X}}]\widehat{\epsilon}_{ij} + \frac{1}{2}\sum_{ijkl} C_{ijkl}[\widehat{\boldsymbol{X}}]\widehat{\epsilon}_{ij}\widehat{\epsilon}_{kl} \tag{14}$$

denotes the pure spontaneous strain-dependent elastic free energy at hydrostatic external stress $\tau_{ij}[\widehat{\boldsymbol{X}}] = -\delta_{ij}P$. For the pure OP potential part, we assume the traditional Landau expansion

$$\Phi(Q;\widehat{\boldsymbol{X}}) = \frac{A[\widehat{\boldsymbol{X}}]}{2}Q^2 + \frac{B[\widehat{\boldsymbol{X}}]}{4}Q^4 + \frac{C[\widehat{\boldsymbol{X}}]}{6}Q^6 + \ldots \tag{15}$$

with P-dependent coefficients yet to be determined. In Ref. [9], it was explicitly shown that the harmonic structure of $\frac{F_0(\underline{\widehat{\epsilon}};\widehat{\boldsymbol{X}})}{V[\widehat{\boldsymbol{X}}]}$ yields the equilibrium spontaneous strain

$$\bar{\widehat{\epsilon}}_{mn} = -\sum_{\nu=1}^{\infty} \bar{Q}^{2\nu} \sum_{ij} d_{ij}^{(2\nu)}[\widehat{\boldsymbol{X}}] S_{mnij}[\widehat{\boldsymbol{X}}] \tag{16}$$

where the compliance tensor $S_{mnij}[\widehat{\boldsymbol{X}}]$ is defined as the tensorial inverse of the so-called *Birch coefficients* [20,21]

$$B_{ijkl}[\widehat{\boldsymbol{X}}] = C_{ijkl}[\widehat{\boldsymbol{X}}] + \frac{1}{2}\left(\tau_{jk}[\widehat{\boldsymbol{X}}]\delta_{il} + \tau_{ik}[\widehat{\boldsymbol{X}}]\delta_{jl} + \tau_{jl}[\widehat{\boldsymbol{X}}]\delta_{ik} + \tau_{il}[\widehat{\boldsymbol{X}}]\delta_{jk} - 2\tau_{ij}[\widehat{\boldsymbol{X}}]\delta_{kl}\right) \tag{17}$$

of the background system $\widehat{\boldsymbol{X}}$ which effectively take over the role of the elastic constants at finite strain. Furthermore, if we eliminate $\bar{\widehat{\epsilon}}_{mn}$ from $\frac{F(Q,\widehat{\epsilon},\widehat{\boldsymbol{X}})}{V[\widehat{\boldsymbol{X}}]}$ by this formula, we obtain the renormalized pure OP potential

$$\begin{aligned}\Phi_R(Q;\widehat{\boldsymbol{X}}) &:= \Phi(Q;\widehat{\boldsymbol{X}}) - \sum_{\mu,\nu=1}^{\infty} \frac{2\mu}{2\mu+2\nu}\left(\sum_{ijkl} d_{ij}^{(2\mu)}[\widehat{\boldsymbol{X}}] S_{ijkl}[\widehat{\boldsymbol{X}}] d_{kl}^{(2\nu)}[\widehat{\boldsymbol{X}}]\right) Q^{2(\mu+\nu)} \\ &\equiv \frac{A_R[\widehat{\boldsymbol{X}}]}{2}Q^2 + \frac{B_R[\widehat{\boldsymbol{X}}]}{4}Q^4 + \frac{C_R[\widehat{\boldsymbol{X}}]}{6}Q^6 + \dots \end{aligned} \tag{18}$$

from which the equilibrium OP $\bar{Q}$ can be determined by minimization.

Information on the P-dependence of elastic constants $C_{ijkl}[\widehat{\boldsymbol{X}}]$ is usually available from density functional theory (DFT) or may be extracted from experimental measurements. At this stage, it therefore remains to relate the potential coefficients $A[\widehat{\boldsymbol{X}}]$, $B[\widehat{\boldsymbol{X}}]$, ... and $d_{ij}^{(2\mu)}[\widehat{\boldsymbol{X}}]$, which are still defined with respect to the reference system $\widehat{\boldsymbol{X}}$ i.e., P-dependent. In a generic application of FSLT, however, one starts from knowledge of an ambient pressure Landau potential, i.e., the lowest order coefficients of the free energy

$$\begin{aligned}\frac{F(Q,\underline{\eta};\boldsymbol{X})}{V(\boldsymbol{X})} &= \Phi(Q;\boldsymbol{X}) + \sum_{\mu=1}^{\infty} Q^{2\mu}\left(\sum_{ij} d_{ij}^{(2\mu,1)}\eta_{ij} + \frac{1}{2!}\sum_{ijkl} d_{ijkl}^{(2\mu,2)}\eta_{ij}\eta_{kl} + \frac{1}{3!}\sum_{ijklmn} d_{ijklmn}^{(2\mu,3)}\eta_{ij}\eta_{kl}\eta_{mn} + \dots\right) \\ &\quad + \frac{1}{2!}\sum_{ijkl} C_{ijkl}^{(2)}\eta_{ij}\eta_{kl} + \frac{1}{3!}\sum_{ijklmn} C_{ijklmn}^{(3)}\eta_{ij}\eta_{kl}\eta_{mn} + \dots \end{aligned} \tag{19}$$

(defined at $\tau_{ij}[\boldsymbol{X}] \equiv 0$) with *P-independent* coefficients are assumed to be known, which obviously places constraints on the possible P-dependence of the above coefficients $A[\widehat{\boldsymbol{X}}]$, $B[\widehat{\boldsymbol{X}}]$, ... and $d_{ij}^{(2\mu)}[\widehat{\boldsymbol{X}}]$. To explore the relations between the two set of coefficients defined in the P-dependent background system $\widehat{\boldsymbol{X}}$ and the laboratory system $\boldsymbol{X}$, we insert the nonlinear superposition relation (11) into (19) and compare coefficients. Following Ref. [9], we content ourselves to just include OP-strain couplings of type $Q^2\widehat{\epsilon}_{ij}$ and obtain

$$A[\widehat{\boldsymbol{X}}] = \frac{1}{J(\alpha)}\left[A[\boldsymbol{X}] + 2\left(\sum_{ij} d_{ij}^{(2,0)}e_{ij} + \frac{1}{2!}\sum_{ijkl} d_{ijkl}^{(2,1)}e_{ij}e_{kl} + \frac{1}{3!}\sum_{ijklmn} d_{ijklmn}^{(2,2)}e_{ij}e_{kl}e_{mn} + \dots\right)\right] \tag{20a}$$

$$d_{st}^{(2)}[\widehat{\boldsymbol{X}}] = \frac{1}{J(\alpha)}\left(\sum_{ij}\alpha_{si}d_{ij}^{(2,0)}\alpha_{tj} + \sum_{ijkl}\alpha_{si}d_{ijkl}^{(2,1)}\alpha_{tj}e_{kl} + \sum_{ijklmn}\alpha_{si}d_{ijklmn}^{(2,2)}\alpha_{tj}e_{kl}e_{mn} + \dots\right) \tag{20b}$$

in addition to the trivial relations $B[\widehat{\boldsymbol{X}}] = B[\boldsymbol{X}]/J(\alpha)$, $C[\widehat{\boldsymbol{X}}] = C[\boldsymbol{X}]/J(\alpha)$, where $J(\alpha) = \det(\alpha_{il})$.

The above parametrization scheme, although mathematically correct, is certainly not very convenient for applications in which the background reference state $\widehat{\boldsymbol{X}}$ is of high symmetry. For the most important example of a cubic high-symmetry phase, the above equations simplify considerable, since the deformation tensor $\alpha_{ij} \equiv \alpha\delta_{ij}$ is diagonal, and so is the Lagrangian background strain $e_{ij} \equiv e\delta_{ij}$ with $e = \frac{1}{2}(\alpha^2 - 1)$, which yields

$$A[\widehat{\boldsymbol{X}}] = \frac{1}{\alpha^3}\left[A[\boldsymbol{X}] + 2\left(e\sum_i d_{ii}^{(2,0)} + \frac{e^2}{2!}\sum_{ik} d_{iikk}^{(2,1)} + \frac{e^3}{3!}\sum_{ikm} d_{iikkmm}^{(2,2)} + \dots\right)\right] \tag{21a}$$

$$d_{st}^{(2)}[\widehat{\boldsymbol{X}}] = \frac{1}{\alpha}\left(d_{st}^{(2,0)} + e\sum_k d_{stkk}^{(2,1)} + e^2\sum_{km} d_{stkkmm}^{(2,2)} + \dots\right) \tag{21b}$$

These formulas are as far as we can get without committing to a specific set of irreducible representations that determine the symmetry-allowed couplings in the Landau potential. Since the background strains $e(P) \sim P + O(P^2)$, they effectively represent a set of highly interrelated power series in powers of P. Unfortunately, this also comes with all the inherent drawbacks. On the one hand, going beyond the lowest order terms, which may be taken from an previously determined ambient pressure Landau potential, we are forced to truncate the above series at rather low order to limit the number of additional unknown parameters. Of course, such truncated series inevitable diverge for increasing values of P. In addition, if we want to employ the theory for the purpose of fitting experimental data, we would like to fix certain experimental observables, in particular the pressure P_0 at which $A_R[\widehat{\boldsymbol{X}}]$ vanishes. Given the above parametrization, this is obviously difficult to do.

In Section 2, we have demonstrated the considerable structural simplification of a standard ambient pressure Landau approach upon replacing Cartesian strain tensors by symmetry-adapted strains. Remarkably, it turns out that, despite the additional complicated nonlinearities contained in formulas (21a) and (21b), similar manipulations may also be carried out in FSLT and are found to yield equally substantial structural simplifications. In the rest of the paper, the resulting scheme will be derived and illustrated by describing the HPPT of KMF.

4. Symmetry-Adapted FSLT: The Cubic-to-Tetragonal HP Phase Transition of KMF

For $\nu = 0, 1, 2 \ldots$, we set

$$\lambda_a^{(\nu)} \equiv \frac{1}{3} \sum_{k_1 \ldots k_\nu} \sum_i d^{(2,\nu)}_{iik_1 k_1 \ldots k_\nu k_\nu} \tag{22a}$$

$$\lambda_t^{(\nu)} \equiv \sum_{k_1 \ldots k_\nu} \frac{d^{(2,\nu+1)}_{33k_1 k_1 \ldots k_\nu k_\nu} - d^{(2,\nu)}_{11k_1 k_1 \ldots k_\nu k_\nu}}{2\sqrt{3}} \tag{22b}$$

in accordance with

$$\lambda_a[\widehat{\boldsymbol{X}}] \equiv \lambda_a(e) \equiv \frac{1}{3} \sum_s d^{(2)}_{ss}[\widehat{\boldsymbol{X}}] \tag{23a}$$

$$\lambda_t[\widehat{\boldsymbol{X}}] \equiv \lambda_t(e) \equiv \frac{d^{(2)}_{33}[\widehat{\boldsymbol{X}}] - d^{(2)}_{11}[\widehat{\boldsymbol{X}}]}{2\sqrt{3}} \tag{23b}$$

Equations (21a) and (21b) are then replaced by

$$\alpha^3 A[\widehat{\boldsymbol{X}}] = A[\boldsymbol{X}] + 6 \sum_{\nu=0}^{\infty} \frac{\lambda_a^{(\nu)}}{(\nu+1)!} e^{\nu+1} \tag{24a}$$

$$\alpha \lambda_{a,t}[\widehat{\boldsymbol{X}}] = \sum_{\nu=0}^{\infty} \lambda_{a,t}^{(\nu)} e^{\nu} \tag{24b}$$

Furthermore, we recall from nonlinear elasticity theory [20] that for a cubic system the compliance tensor $S_{ijkl}[\widehat{\boldsymbol{X}}]$ and the bulk modulus $K[\widehat{\boldsymbol{X}}] = (B_{1111}[\widehat{\boldsymbol{X}}] + 2B_{1122}[\widehat{\boldsymbol{X}}])/3$ at finite pressure are related by $\sum_i S_{iijj}[\widehat{\boldsymbol{X}}] = S_{1111}[\widehat{\boldsymbol{X}}] + 2S_{1122}[\widehat{\boldsymbol{X}}] = 1/3K[\widehat{\boldsymbol{X}}]$, while, for the longitudinal shear modulus, $\mu[\widehat{\boldsymbol{X}}] = (B_{1111}[\widehat{\boldsymbol{X}}] - B_{1122}[\widehat{\boldsymbol{X}}])/2$ the relation $S_{1111}[\widehat{\boldsymbol{X}}] - S_{1122}[\widehat{\boldsymbol{X}}] = 1/2\mu[\widehat{\boldsymbol{X}}]$ holds. If we replace the Cartesian

equilibrium spontaneous strain components (16) by their symmetry-adapted volume and tetragonal counterparts using these relations, they acquire the representations

$$\bar{\epsilon}_a = -\frac{\lambda_a[\widehat{\boldsymbol{X}}]}{K[\widehat{\boldsymbol{X}}]}\bar{Q}^2, \qquad \bar{\epsilon}_t = -\frac{2\lambda_t[\widehat{\boldsymbol{X}}]}{\mu[\widehat{\boldsymbol{X}}]}\bar{Q}^2 \tag{25}$$

Furthermore, it is easy to check the identity

$$\sum_{ijkl} d_{ij}^{(2)}[\widehat{\boldsymbol{X}}] S_{ijkl}[\widehat{\boldsymbol{X}}] d_{kl}^{(2)}[\widehat{\boldsymbol{X}}] = \frac{\lambda_a^2[\widehat{\boldsymbol{X}}]}{K[\widehat{\boldsymbol{X}}]} \tag{26}$$

which allows for similarly rewriting the renormalized potential $\Phi_R(Q;\widehat{\boldsymbol{X}})$ as

$$\Phi_R(Q;\widehat{\boldsymbol{X}}) = \Phi(Q;\widehat{\boldsymbol{X}}) - \frac{Q^4}{4}\left(\frac{2\lambda_a^2[\widehat{\boldsymbol{X}}]}{K[\widehat{\boldsymbol{X}}]} + \frac{8\lambda_t^2[\widehat{\boldsymbol{X}}]}{\mu[\widehat{\boldsymbol{X}}]}\right) \tag{27}$$

Combining these equations with Equations (24a) and (24b), we can summarize the symmetry-adapted parametrization of the coefficients of the renormalized Landau potential (18), whose minimization determines the equilibrium OP $\bar{Q}$ with

$$A_R[\widehat{\boldsymbol{X}}] = \frac{A[\boldsymbol{X}]}{\alpha^3} + \frac{6\Delta_a[\widehat{\boldsymbol{X}}]}{\alpha^3} \tag{28a}$$

$$B_R[\widehat{\boldsymbol{X}}] = \frac{B[\boldsymbol{X}]}{\alpha^3} - \frac{2(\lambda_a^{(2)}[\widehat{\boldsymbol{X}}])^2}{K[\widehat{\boldsymbol{X}}]} - \frac{8\lambda_t^2[\widehat{\boldsymbol{X}}]}{\mu[\widehat{\boldsymbol{X}}]} \tag{28b}$$

in addition to $C_R[\widehat{\boldsymbol{X}}] = \widetilde{C}[\widehat{\boldsymbol{X}}]$, where we introduced the function

$$\Delta_a[\widehat{\boldsymbol{X}}] \equiv \Delta_a(e) \equiv \sum_{\nu=0}^{\infty} \frac{\lambda_a^{(\nu)}}{(\nu+1)!} e^{\nu+1} \tag{29}$$

Note the close formal similarity of Equations (28a), (28b) and (29) with their infinitesimal counterparts (7a) and (7b). In a generic application of this theory with cubic high symmetry, the lowest order Landau coefficients $A[\boldsymbol{X}], B[\boldsymbol{X}], C[\boldsymbol{X}]$ and the lowest order strain-OP coupling coefficients $\lambda_{a,t}^{(0)}$ can be taken from an existing ambient pressure Landau theory. Furthermore, the (diagonal) background deformation components $\alpha = \alpha(P)$ and the resulting Lagrangian strain $e = e(P)$ may be determined by fitting a suitable EOS to the cubic unit cell volume data. Such a fit also immediately yields the pressure-dependent bulk modulus $K[\widehat{\boldsymbol{X}}] \equiv K(P)$. It is only for the pressure-dependence of the longitudinal shear modules $\mu[\widehat{\boldsymbol{X}}] = \mu(P)$ that we are truly forced to resort to additional input from DFT. To determine the EOS and the elastic constants of $KMnF_3$, we have performed a series of fairly standard DFT calculations. We refer to Appendix A for further details of these simulations.

Since we do not need to maintain the highest possible precision in determining $\mu(P)$ at room temperature but can content ourselves with a reasonable approximation, we use the following heuristic strategy to promote the DFT result $\mu_{\mathrm{DFT}}(P)$ from $T = 0$ to ambient temperature. Figure 7 shows a comparison of the bulk moduli $K_{\mathrm{DFT}}(P)$ calculated from DFT to the result for $K(P)$ obtained from the Murnaghan fit of the data published in Ref. [11]. Numerically, one finds the fraction of these moduli stays

entirely within the narrow bounds $0.918 \leq K(P)/K_{\mathrm{DFT}}(P) \leq 0.92$ over the whole interval $0 \leq P \leq 20$ GPa. We therefore postulate a similar behavior for $\mu(P)$, setting

$$\mu(P) \equiv \frac{K(P)}{K_{\mathrm{DFT}}(P)} \cdot \mu_{\mathrm{DFT}}(P) \tag{30}$$

Figure 8 illustrates the resulting behavior of $\mu(P)$.

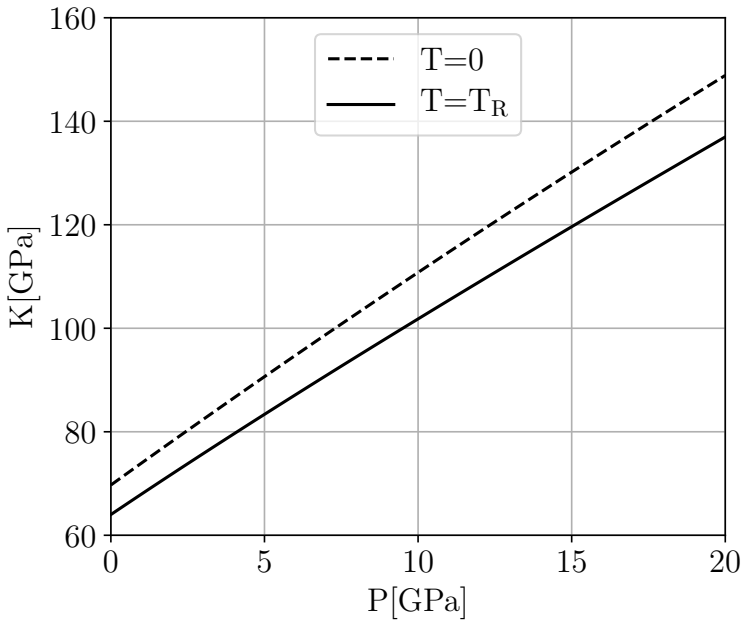

Figure 7. Comparison of pressure-dependent bulk modulus $K(P)$ at room temperature $T = T_R$ extracted from the Murnaghan fit of the cubic part of the unit cell data of Ref. [11] to the $T = 0$ result obtained from DFT.

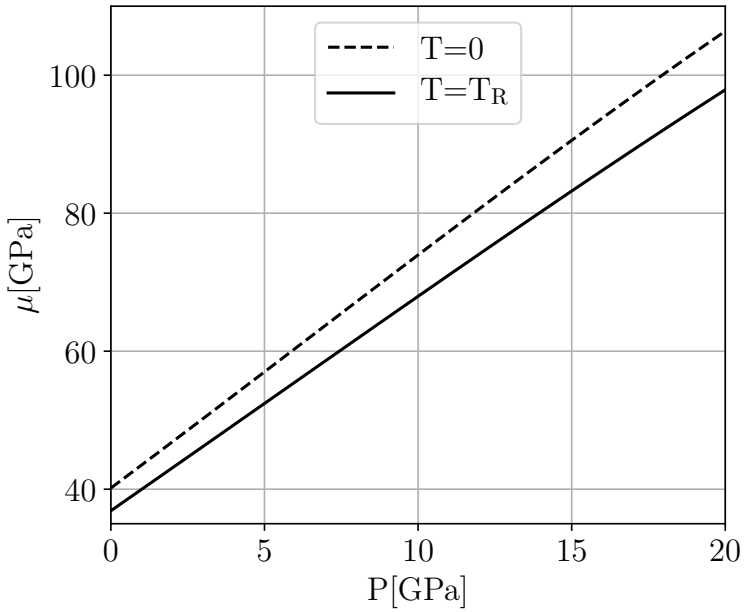

Figure 8. Pressure-dependent longitudinal shear modulus $\mu(P)$ at room temperature $T = T_R$ as determined by extrapolating the corresponding DFT result from $T = 0$ to $T = T_R$ based on Formula (30).

With all other ingredients in place, this leaves only the higher order coefficients $\lambda_{a,t}^{(\nu)}, \nu > 0$ as the remaining undetermined parameters of FSLT. It therefore seems that these parameters must be treated as unknown fit parameters in a practical application. In the next section, however, we will introduce a much more convenient and powerful approach.

5. Efficient Parametrization

Comparing the above symmetry-adapted system of equations to what we had before, a considerable structural simplification is obvious. However, the following drawbacks seem to persist:

- Truncating the functions $\lambda_{a,t}[\widehat{\boldsymbol{X}}]$ defined by Equation (24b) at finite order $e^\nu = e^\nu(P)$ still results in divergent behavior with increasing P.
- In addition to a given set of strain measurements which we would want to feed to least squares fits based on Landau theory, rather accurate experimental information on the critical temperature T_c or the critical pressure P_c is frequently available from complementary experimental measurements. Unfortunately, least squares fitting procedures of strain measurements with an unconstrained value of T_c or P_c frequently tend to displace T_c or P_c and thus degrade the accuracy of the fit in the transition region. At least for a second order transition, the critical point is, of course, determined by the zero of the quadratic coefficient A_R of the Landau expansion. Therefore, we would like to be able to explicitly constrain the behavior of A_R, possibly fixing both its zero and/or slope at zero as a function of T or P. Unfortunately, based on a set of interrelated truncated power series, this is still hard to do.

In what follows, we propose a new scheme which finally allows for practically overcoming all of these problems in a single push. Let us start by taking a second look at Figure 6. Of course, the correct functional form of $A_R[\widehat{\boldsymbol{X}}] \equiv A_R(T_R, P)$ that we are looking for should be that of a well-behaved function passing through zero around $P_c \approx 4$ GPa. At $P = 0$, however, it should start out with roughly twice the initial slope of the purely linear yellow curve if we are to retain the ambient pressure Landau parameters. The pressure dependence of the correct function $A_R(T_R, P)$ must therefore be far from linear. Experimentally, there is no indication of a re-entrant behavior below 25GPa, so we do not expect any second crossing point in this pressure range. Unfortunately, our numerical tests quickly revealed that, using a truncated version of $\Delta_a(e(P))$ as defined in (29), it seems virtually impossible to meet these requirements unless one is willing to go to prohibitively high truncation order, thus introducing a plethora of unknown fit parameters and the accompanying horrific numerical problems.

A way out is to propose a reasonable function $\Delta_a(e(P))$ in closed form that meets all of the above requirements while still containing some adjustable parameters that offer a certain amount of variational flexibility to allow improvement by least squares fitting. Of course, there are many ways to do this, and the choices are only limited by the reader's ingenuity. In fact, since the summand $\nu = 0$ of $\Delta_a(x)$ contributes the lowest order coefficient $x\lambda_a^{(0)}$, which is usually fixed from knowledge of an existing ambient pressure Landau theory, all candidate functions $\Delta_a(x)$ that start out like

$$\Delta_a(x) = \lambda_a^{(0)} x + O(x^2) \tag{31}$$

qualify as candidates for a meaningful function $\Delta_a(x)$. In our current application to KMF, we parametrize

$$A_R \equiv A_R(T_R, e(P)) = \frac{A_R(T_R) + 6\Delta(e(P); b, c, d)}{\alpha^3(P)} \tag{32}$$

by introducing the function

$$\Delta(e; b, c, d) := ce + 2bf_d(e) \tag{33}$$

with parameters b, c, d combining a linear part with slope c and a nonlinear contribution $f_d(e)$, which remains yet to be specified. Our general parametrization strategy is then as follows:

- As a function of e, $A_R(T_R, e)$ should start out with slope $s = -6\lambda_a^{(0)} \equiv c + 2bf_d'(0)$, so parameter b can be traded for the slope s of $\Delta(e; b, c, d)$ at $e = 0$.
- Suppose further that $A_R(T_R, e)$ should vanish at a critical value $e_0 = e(P_0)$ of the background strain e. For $\Delta(e; b, c, d)$, this implies the constraint equation $\alpha + \Delta(e_0; b, c, d) \equiv 0$ where $\alpha \equiv A_R(T_R, 0)/6$, which may be solved for parameter c.

These steps eliminate parameters b, c in favor of the constants α and e_0, leaving d as the single remaining free variational parameter. We still need to reconcile this parametrization of A_R with that of the function $\lambda_a[\widehat{\boldsymbol{X}}]$ as defined in Equation (24b). We focus on the power series part

$$\Lambda(x) \equiv \sum_{\nu=0}^{\infty} \lambda_a^{(\nu)} x^\nu \tag{34}$$

which is based on the same set of coefficients $\lambda_a^{(\nu)}$ as $\Delta_a(x)$ but lacks the accompanying factorials $1/\nu!$. These factorials can, however, easily be taken care of. Observe that

$$\int_0^\infty dt\, e^{-t} \frac{(tx)^{\nu+1}}{(\nu+1)!} = x^{\nu+1} \tag{35}$$

Therefore, using the *Borel transform*

$$(\mathcal{B}\Delta)(x) \equiv \int_0^\infty dt\, e^{-tx} \Delta(tx) \tag{36}$$

we may relate

$$\Lambda(x) = \frac{(\mathcal{B}\Delta)(x)}{x} \tag{37}$$

It remains to specify a suitable function $f_d(x)$. Beyond producing a reasonable function $A_R(T_R, e)$, the job profile for recruiting such a function includes at least two basic requirements:

- It would be highly desirable to be able to compute the corresponding Borel transform $(\mathcal{B}f_d)(x)$ in closed form.
- $f_d(x)$ should also allow for solving the equation $\alpha + \Delta(e_0; b, c, d) \equiv 0$ explicitly.

For the present goal of understanding the HPPT in KMF, we came up with the choice

$$f_d(e) := -1 + \sqrt{1 - d^2 e} \tag{38}$$

(note that $e(P) < 0$ for $P > 0$) which meets both of these minimal requirements, since, in this case, $b = (c - s)/d^2$ and

$$c = \frac{s\left(\sqrt{1 - d^2 e_0} - 1\right) - \alpha d^2/2}{d^2 e_0/2 + \sqrt{1 - d^2 e_0} - 1} \tag{39}$$

In this way, we have completely bypassed Taylor series expansions and their various accompanying drawbacks. Figure 9 illustrates the remaining variational freedom in our chosen parametrization.

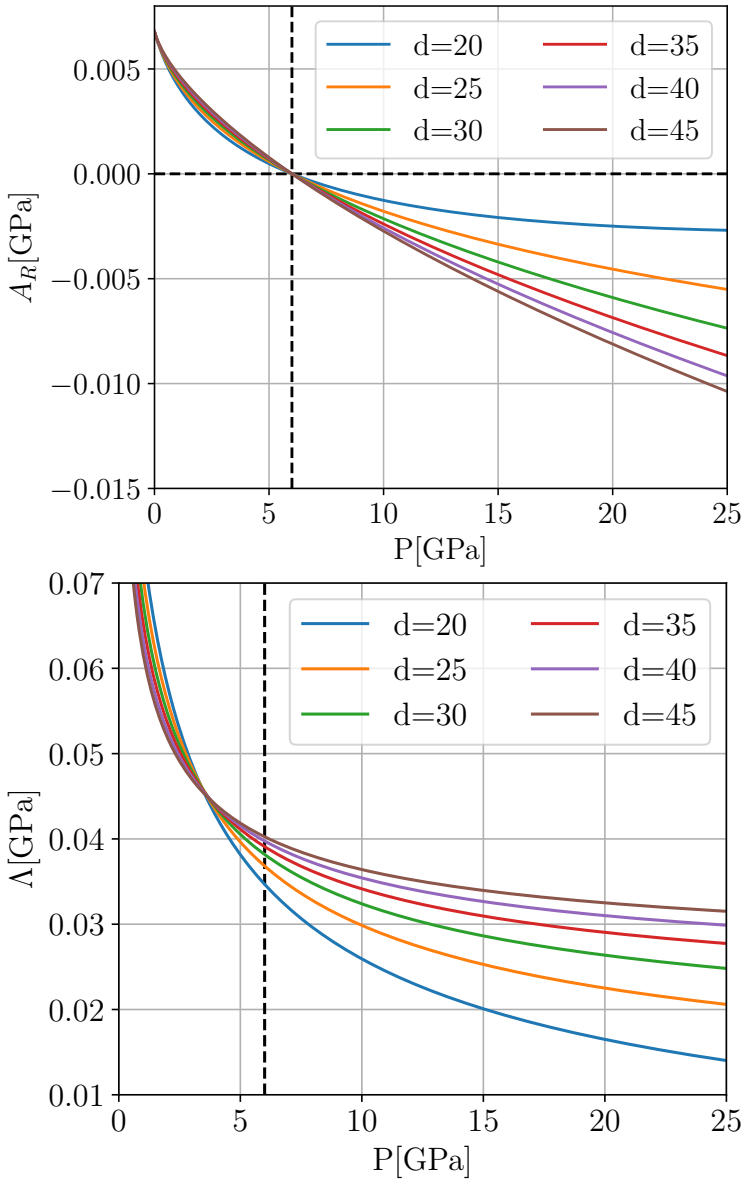

Figure 9. Illustration of the remaining d-dependence of the parametrization of $A_R(T_R, e(P))$ by Equation (32) (upper panel) and the resulting function $\Lambda(e(P))$ as given by the Borel transform Equation (37) (lower panel). Parameters b and c were eliminated in favor of parameter $\lambda_a^{(0)} = 0.128$ GPa as prescribed from ambient pressure LT and a chosen pressure parameter $P_0 = 6.0$ GPa.

In summary, at this stage, the function $\Delta_a[\widehat{\boldsymbol{X}}]$ which governs the behavior of $A_R[\widehat{\boldsymbol{X}}]$ and—through a Borel transform—also provides the coupling function $\lambda_a[\widehat{\boldsymbol{X}}]$ between the spontaneous volume strain $\bar{\tilde{\epsilon}}_a$ and $\bar{Q}^2$ according to Equation (25) has been specified up to a single free parameter d. The remaining coupling function $\lambda_a[\widehat{\boldsymbol{X}}] \equiv \lambda_a(P)$ explicitly determines the proportionality between the spontaneous tetragonal strain $\bar{\tilde{\epsilon}}_a$ and $\bar{Q}^2$, However, both $\lambda_a[\widehat{\boldsymbol{X}}]$ and $\lambda_t[\widehat{\boldsymbol{X}}]$ also enter implicitly into the spontaneous strain via its implicit dependence on the quartic coefficient $B_R[\widehat{\boldsymbol{X}}]$ of the renormalized Landau potential as given by Equation (28b), and, apart from the reasonable requirement $\lim_{P\to 0} \lambda_t[\widehat{\boldsymbol{X}}] = \lambda_t^{(0)}$, nothing is known in advance about its pressure dependence, such that introducing a truncated Taylor series and least squares

fitting seems unavoidable. However, we can actually do a lot better than this. Let us consider experimental high pressure spontaneous strain data in the form of n data points $(P_i, \widehat{\epsilon}_{a,\mathrm{exp}}(P_i), \widehat{\epsilon}_{a,\mathrm{exp}}(P_i))_{i=1}^{n}$. In fact, at a given prescribed pressure value P_i and with all other parameters in place, we can regard the room temperature values $\widehat{\epsilon}_a = \widehat{\epsilon}_a(\lambda_t(P_i))$ and $\widehat{\epsilon}_t = \widehat{\epsilon}_t(\lambda_t(P_i))$ as functions of the-unknown-function values $\lambda_t(P_i)$. The "best" value $\lambda_t(P_i)$ matching the data point $(P_i, \widehat{\epsilon}_{a,\mathrm{exp}}(P_i), \widehat{\epsilon}_{a,\mathrm{exp}}(P_i))$ may then be determined by numerically minimizing the function

$$\begin{aligned} s_i(\lambda_t(P_i)) \quad := \quad & w_a \left[\widehat{\epsilon}_{a,\mathrm{exp}}(P_i) - \widehat{\epsilon}_a(\lambda_t(P_i))\right]^2 \\ & + w_t \left[\widehat{\epsilon}_{t,\mathrm{exp}}(P_i) - \widehat{\epsilon}_t(\lambda_t(P_i))\right]^2 \end{aligned} \tag{40}$$

with weights w_a, w_t suitable adjusted to counterbalance size differences between $\widehat{\epsilon}_a$ and $\widehat{\epsilon}_t$. Carried out for all $i = 1, \ldots, n$, this prescription results in a collection of n "optimal" values $\lambda_t(P_i)$ from which one may hope to recover the full function $\lambda_t(P)$ by interpolation. Figure 10 shows the result of our corresponding effort for KMF. Amazingly, we observe that all values $\lambda_t(P_i)$ seem to accumulate on a straight line whose extrapolation $P \to 0$ perfectly passes through the point $(0, \lambda_t^{(0)})$, which is just the limiting value imposed by ambient pressure Landau theory. We believe that this behavior is not coincidental but a strong indication that the present parametrization is internally consistent and correct.

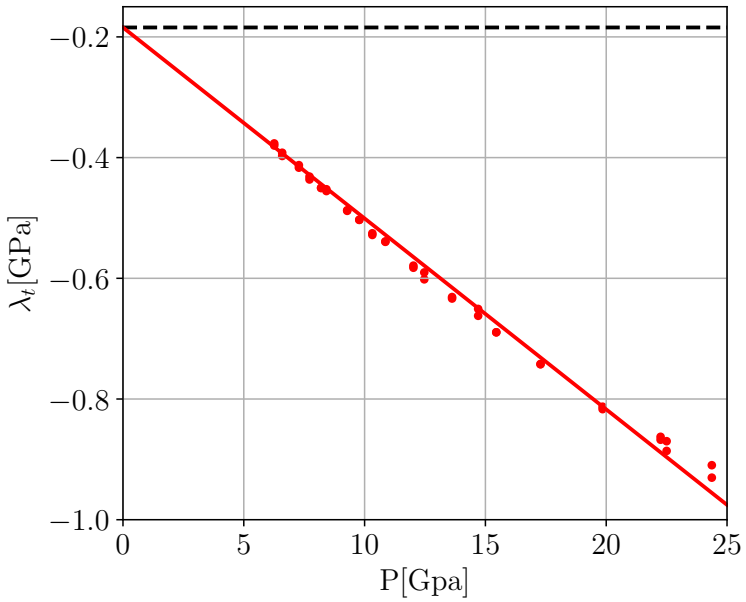

Figure 10. Results of minimizing the sum (40) using the relative weights $(w_a, w_t) = (10, 1)$ and pressure parameters $P_0 = 6$GPa, $d = 40$. The dashed horizontal line indicates the limiting value $\lambda_t(P = 0) \equiv \lambda_t^{(0)}$.

A simple linear fit of $\lambda_t(P)$ therefore completes our Landau parametrization. Our results for the pressure dependence of the couplings $A_R(P), \widetilde{B}(P), \lambda_{a,t}(P)$ and the resulting pressure dependence of the equilibrium OP $\bar{Q}(P)$ are illustrated in Figure 11. Note that in the present description the transition appears to be of first rather than second order, with $P_0 = 6\,\mathrm{GPa}$ yielding a transition pressure $P_c \approx 4.5\,\mathrm{GPa}$. Finally, the resulting parametrization of the spontaneous strain is compared to experiment in Figure 12.

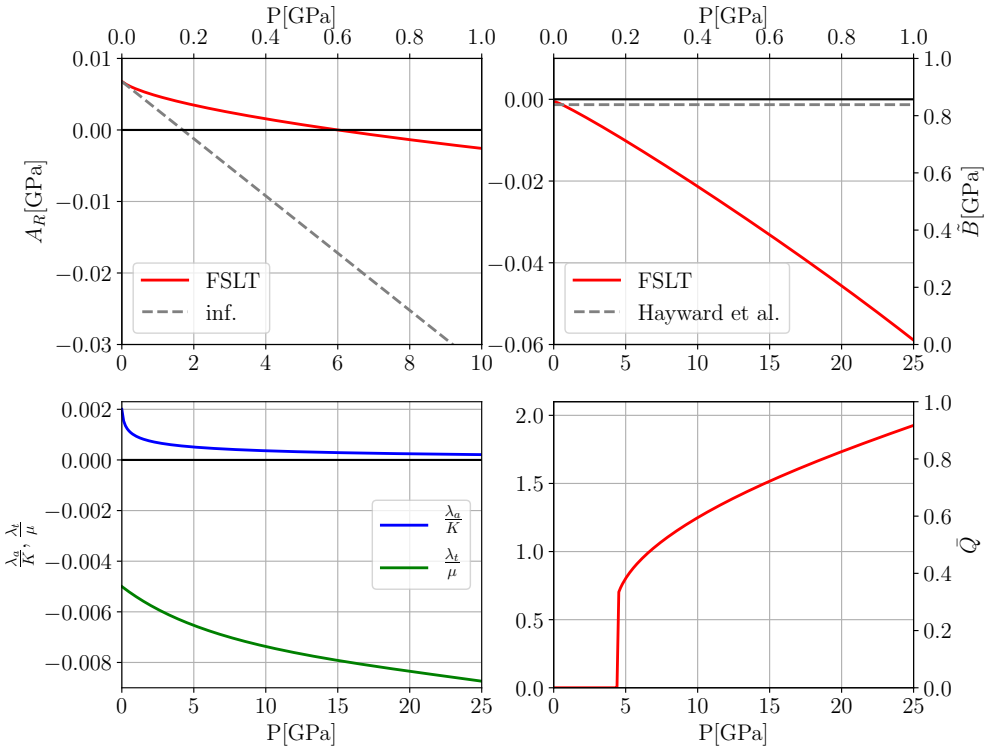

Figure 11. Upper left panel: pressure dependence of Landau parameters $A_R(P)$ as compared to the simple linear behavior of infinitesimal strain LT assumed in Equation (7a). Upper right panel: pressure dependence of $\tilde{B}(P)$. The dashed horizontal line indicates the corresponding value from the parametrization of Hayward et al. [19] taken at $T = 186.5$ K, which is slightly displaced from our limiting value at $P = 0$ since we are taking into account thermal softening of $K(P)$ and $\mu(P)$ for room temperature. Lower left panel: pressure dependence of coupling parameters $\lambda_a(P)/K(P)$ and $\lambda_t(P)/\mu(P)$. Lower right panel: resulting behavior of the equilibrium order parameter $\bar{Q}(P)$ (right).

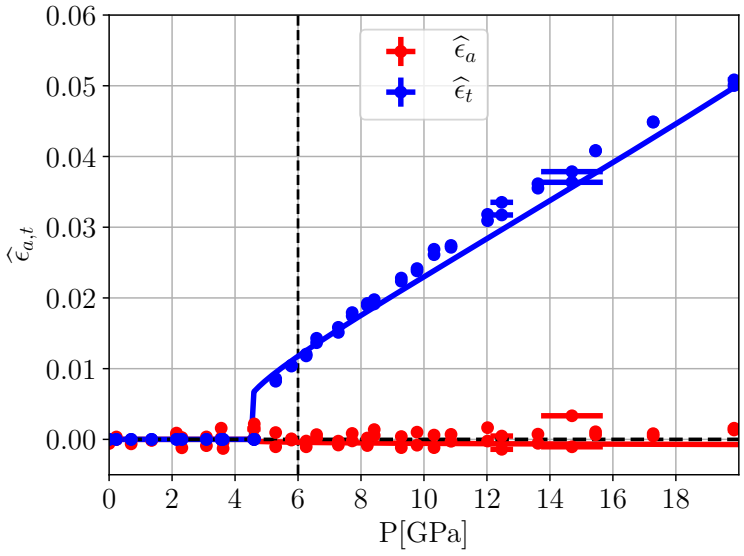

Figure 12. Parametrization of spontaneous strains $\widehat{\epsilon}_a, \widehat{\epsilon}_t$ in comparison to experimental data from Ref. [11]. The thin vertical line indicates the pressure parameter $P_0 = 6$ GPa.

6. Discussion

For the high pressure community, our present paper contains some good news and some bad news—first, the bad news. We hope to have demonstrated convincingly that classical Landau theory is usually completely inadequate for "explaining" experimental findings in the field of high pressure phase transitions, and the conclusions drawn from it will often be misleading at best. Taking the example of KMF, both the first order character of the transition and the correct value of the transition pressure are completely obscured by sticking to Landau theory with infinitesimal strain coupling, even if one is willing to distort a pre-existing ambient pressure Landau parametrization beyond recognition. The good news, however, is that with the development of FSLT a mathematically consistent alternative incorporating nonlinear elasticity has recently become available. Up to now, however, FSLT has been rather complicated in structure, which quite likely scared off many potential users and thus did not lead to the widespread use that its developers were initially hoping for. The present paper, which exploits the enormous simplifications that arise by passing (i) from Cartesian to symmetry-adapted finite strains and (ii) by virtue of (i), from truncated Taylor expansions to a functional parametrization. These improvements should pave the way for routine use of our theory in successfully describing HPPTs. In particular, the present paper illustrates that, while the former version of FSLT involved delicate least-squares fitting procedures with a large number of unknown fit parameters and dealing with all the inadequacies implicit in the use of truncated Taylor expansions, in the present scheme, the unknown pressure dependencies can be systematically determined one-by-one in a step-wise, almost "deterministic" manner.

Admittedly, even the present parametrization of the HPPT in KMF is still less than perfect. For instance, the coupling function $\lambda_a(P)/K(P)$ shown in the lower left panel of Figure 11 exhibits a steep initial decrease with increasing pressure. Since no spontaneous strain data are available for this pressure region, this does not change the physical values produced by the theory. However, it hints at a sub-optimal choice Equation (38) for the auxiliary function $f_d(x)$. The reader is invited to come up with an improved candidate function.

More importantly, in a full-blown application of FSLT, we should be able to predict e.g., the (P,T) cubic-to-tetragonal phase boundary of KMF and compute pressure—and temperature-dependent elastic constants. In principle, the ability to do so depends mainly on the successful construction of a pressure—and temperature-dependent baseline, i.e., the cubic EOS $V_{\text{cubic}} = V_{\text{cubic}}(P,T)$. In a previous paper [10], this task has been successfully carried out for the perovskite $PbTiO_3$ by combining zero temperature DFT calculations (see Appendix A for details) with the Debye approximation as implemented in the GIBBS2 package [22,23] to incorporate effects of thermal expansion (recently, we learned [24] that a similar approach also seems to work for $MgSiO_3$). Unfortunately, our corresponding efforts to derive $V_{\text{cubic}}(P,T)$ for KMF along the same lines have failed so far, however. This failure manifests itself e.g., in the inability to simultaneously reproduce the thermal baseline at $P = 0$ measured experimentally and the ambient temperature EOS, even if we allowed for the introduction of a constant compensating background pressure which is frequently introduced in DFT calculations to compensate inadequacies of an employed exchange-correlation functional. Ref. [25] states that perovskites with octahedral tilting generally do not show an appreciable coupling between structural and magnetic order parameters. Nevertheless, this statement obviously does not exclude effects due to a coupling between magnetic degrees of freedom and the background volume strain. Since the Debye approximation is based exclusively on phonons, we may speculate that in KMF residual magnetic effects may be responsible for additional thermal energy consumption. An investigation of this problem is currently underway.

Finally, it may be argued that our current theory also does not "explain" the origins of the involved nonlinear P-dependencies on a fundamental level. In approaches based on infinitesimal strain couplings, similarly looking P-dependent couplings are also introduced, but in a more or less completely ad hoc

manner, blaming their existence on rather unspecific "higher order strain couplings". As a rule, such an approach results in a mathematically inconsistent theory. In contrast, the nonlinearities that arise in FSLT result for different but well-defined reasons. On the one hand, there are couplings between powers of the background strain $e(P)$ and the Landau potential $\Phi_R(Q;\widehat{\mathbf{X}})$ "floating" on this background strain, and there is a pressure-dependence of the elastic moduli $K(P)$ and $\mu(P)$, which is in principle accessible e.g., to DFT calculations. This leaves the task of "explaining" the residual nonlinearities in the functions $\lambda_{a,t}(P)$ describing the couplings between order parameter and spontaneous strains. In contrast to blaming their existence on the effects of some unspecified higher order couplings, our present theory provides a practical way to numerically determine these functions. In addition, we see no reason in principle as to why such P-dependent coupling constants could not eventually be extracted from DFT calculations along the general philosophy laid out in Refs. [26,27] and the subsequent follow-up literature.

Author Contributions: A.T.: concept, main theory, and writing; W.S.: additional theory, comparison to previous experimental data; S.E., K.B., and P.B.: DFT calculations. All authors have read and agreed to the published version of the manuscript.

Funding: A.T., S.E., and K.B. acknowledge support by the Austrian Science Fund (FWF) Project P27738-N28. W.S. acknowledges support by the Austrian Science Fund (FWF) Project P28672-N36. S.E. acknowledges support from H.E.C., Pakistan.

Acknowledgments: A.T. would like to thank Ronald Miletich-Pawliczek for useful discussions.

Conflicts of Interest: The authors declare no conflict of interest.

Abbreviations

The following abbreviations are used in this manuscript:

AFN	antiferromagnetic
DFT	density functional theory
EOS	equation of state
FSLT	finite strain Landau theory
HPPT	high pressure phase transition
KMF	$KMnF_3$
LDA	local density approximation
LT	Landau theory
OP	order parameter
PT	phase transition
NM	nonmagnetic

Appendix A. DFT Calculation Details

The EOS and the elastic constants in the cubic phase of KMF were calculated using the WIEN2K DFT package, which is an all-electron code based on the (linearized) augmented plane-wave and local orbitals [(L)APW+lo] basis representation of the Kohn–Sham equations [28] of DFT. Here, we only content ourselves with a quick outline of the basic ideas and refer to Refs. [29,30] and the monograph Ref. [31] for more details.

In the (L)APW+lo method, the crystal's unit cell is partitioned into a set of atomic spheres surrounding the nuclei and a remaining interstitial region. Inside these atomic spheres, the wave functions are expanded into atomic-like basis functions, i.e., numerical radial functions times spherical harmonics while they are represented by plane waves throughout the interstitial region. These two regions are glued together by requiring continuity of the basis functions in value (and, depending on the flavor of the (L)APW+lo method, in radial slope) across the sphere boundaries. These LAPW calculations require making a couple

of choices regarding cell size, standard parameter values, etc. In detail, the calculations of the present work were done with $R_{\mathrm{MT}}^{\mathrm{min}} K_{\mathrm{max}} = 9$ and atomic sphere radii of 2.1, 2.0, and 1.6 bohr for K, Mn and F, respectively. The energy separation between core and valance states used was -6.0 Ry. Inside the sphere, the maximum angular momentum used in the spherical expansions was L_{max} = 10, while the charge density in the interstitial was Fourier expanded up to a cutoff of $G_{\mathrm{max}} = 14(a.u.)^{-1}$.

As to the use of exchange-correlation functionals, we have performed calculations using the standard local density approximation (LDA) [32] and three functionals of the generalized gradient approximation, namely, PBE from Perdew et al. [33,34], its solid-state optimized version PBEsol [35], and WC from Wu and Cohen [36]. For LDA and PBE, we observed the well-known tendency to underestimate and overestimate the lattice constants of solids, respectively, while PBEsol and WC produced more accurate results in between LDA and PBE [37,38].

To study the effect of magnetism on our results, we undertook calculations for a standard non-magnetic (NM) and ferromagnetic (FM) cubic perovskite unit cell with five atoms as well as an for a cubic supercell with 10 atoms in antiferromagnetic (AFM) structures of A-type, C-type and G-type [39]. After sufficient testing, we settled for a k-mesh sampling of $10 \times 10 \times 10$ k-points for all types of structures. In FM and AFM structure, we observed a linearization error which is inherent to the basis functions inside the spheres. To overcome this problem, we use the second energy derivative of the radial part (HDLO) for d electrons for Mn atom (for more detail see Ref. [40]). Using this setup, we identified that G-type AFM structure to have lowest energy.

Cubic elastic elastic constants were calculated with the help of the WIEN2K add-on package by Charpin [41]. Results at $T = 0$ are compiled in Table A1. In particular, we conclude that FM and AFM structures give similar value of lattice parameters and bulk modulus, which suggests that the specific magnetic ordering is not overly important for these quantities. In passing, we note that non-magnetic KMF is found to be a metal (with all functionals), but all magnetic structures lead to insulators (with all functionals). Simulations with PBEsol+U with U = 4eV in the AFM G-type phase would even lead to slightly better agreement with experiment for lattice constants and bulk modulus, but overall the effect is small and we therefore used the PBEsol results in Figures 7 and 8.

Table A1. Lattice constant (Å) and bulk modulus (GPa) of cubic $KMnF_3$ for different methods used in this work.

	Present Work			**Other Works**	
	NM	**FM**	**AFM (G-Type)**	**PBE**	**Expt.**
Lattice constant					4.185 [42]
LDA	3.89	4.11	4.09		
PBEsol	3.96	4.19	4.17		
PBE	4.04	4.26	4.24	4.19 [43]	
PBEsol + U (U = 4 ev)		4.20	4.19		
Bulk modulus					
LDA	117.2	83.7	88.4		
PBEsol	97.6	70.4	69.6		
PBE	83.3	62.3	63.1		
PBEsol + U (U=4 ev)		68.2	67.7		

Estimating an additional softening due to finite temperature with various flavors of the Debye approximation which are implemented in the GIBBS2 software [22,23], the best agreement with the cubic part of the experimental data of Ref. [11] was reached for the combination of G-type antiferromagnetic structure and PBEsol functional.

References

1. Landau, L.; Lifshitz, E.; Pitaevskii, L. *Statistical Physics Part I*; Butterworth and Heinemann: Oxford, UK, 2001.
2. Tolédano, J.; Tolédano, P. *The Landau Theory of Phase Transitions*; World Scientific: Singapore, 1987.
3. Rabe, K.; Ahn, C.; Triscone, J.M. (Eds.) Physics of Ferroelectrics. In *Topics in Applied Physics*; Springer: Berlin/Heidelberg, Germany, 2007; Volume 105.
4. Salje, E. *Phase Transitions in Ferroelastic and Coelastic Crystals*; Cambridge University Press: Cambridge, UK, 1990.
5. Tröster, A.; Schranz, W.; Miletich, R. How to Couple Landau Theory to an Equation of State. *Phys. Rev. Lett.* **2002**, *88*, 055503. [CrossRef]
6. Koppensteiner, J.; Tröster, A.; Schranz, W. Efficient parametrization of high-pressure elasticity. *Phys. Rev. B* **2006**, *74*, 014111. [CrossRef]
7. Schranz, W.; Tröster, A.; Koppensteiner, J.; Miletich, R. Finite strain Landau theory of high pressure phase transformations. *J. Phys. Condens. Matter* **2007**, *19*, 275202. [CrossRef]
8. Tröster, A.; Schranz, W. Landau theory at extreme pressures (invited paper for contribution to the special edition of "FERROELECTRICS") (birthday edition in honour of V. Ginzburg's 90th birthday). *Ferroelectrics* **2007**, *354*, 208. [CrossRef]
9. Tröster, A.; Schranz, W.; Karsai, F.; Blaha, P. Fully Consistent Finite-Strain Landau Theory for High-Pressure Phase Transitions. *Phys. Rev. X* **2014**, *4*, 031010. [CrossRef]
10. Tröster, A.; Ehsan, S.; Belbase, K.; Blaha, P.; Kreisel, J.; Schranz, W. Finite-strain Landau theory applied to the high-pressure phase transition of lead titanate. *Phys. Rev. B* **2017**, *95*, 064111. [CrossRef]
11. Guennou, M.; Bouvier, P.; Garbarino, G.; Kreisel, J.; Salje, E. Pressure-induced phase transition(s) in $KMnF_3$ and the importance of the excess volume for phase transitions in perovskite structures. *J. Phys. Condens. Matter* **2011**, *23*, 485901. [CrossRef]
12. Carpenter, M.A.; Becerro, A.I.; Seifert, F. Strain analysis of phase transitions in (Ca, Sr) TiO_3 perovskites. *Am. Mineral.* **2001**, *86*, 348–363. [CrossRef]
13. Salje, E.K.H.; Zhang, M.; Zhang, H. Cubic–tetragonal transition in $KMnF_3$: IR hard-mode spectroscopy and the temperature evolution of the (precursor) order parameter. *J. Physics: Condens. Matter* **2009**, *21*, 335402.
14. Dormann, E.; Copley, J.R.D.; Jaccarino, V. Temperature dependence of the MnF_2 and $KMnF_3$ lattice parameters from room temperature to the melting point. *J. Phys. C Solid State Phys.* **1977**, *10*, 2767–2771. [CrossRef]
15. Ratuszna, A.; Pietraszko, A.; Chelkowski, A.; Lukaszewicz, K. The Temperature Dependence of Lattice Parameters of KMeF3 and KMn0.9Me0.1F3 Compounds (Me = Mn2+, Co2+, and Ni2+). *Phys. Status Solidi (a)* **1979**, *54*, 739–743. [CrossRef]
16. Sakashita, H.; Ohama, N. A precursor effect in the lattice constant at the 186 K-structural phase transition in KMnF3. *Phase Transit.* **1982**, *2*, 263–276. [CrossRef]
17. Sakashita, H.; Ohama, N.; Okazaki, A. Thermal expansion and spontaneous strain of KMnF3 near the 186 K-structural phase transition. *Phase Transit.* **1990**, *28*, 99–106. [CrossRef]
18. Gibaud, A.; Shapiro, S.M.; Nouet, J.; You, H. Phase diagram of $KMn_{1-x}Ca_xF_3$ ($x < 0.05$) determined by high-resolution X-ray scattering. *Phys. Rev. B* **1991**, *44*, 2437–2443. [CrossRef]
19. Hayward, S.A.; Romero, F.J.; Gallardo, M.C.; del Cerro, J.; Gibaud, A.; Salje, E.K.H. Cubic-tetragonal phase transition in KMnF3: Excess entropy and spontaneous strain. *J. Phys. Condens. Matter* **2000**, *12*, 1133–1142. [CrossRef]
20. Wallace, D. *Thermodynamics of Crystals*; Dover: New York, NY, USA, 1998.
21. Morris, J.W.; Krenn, C.R. The internal stability of an elastic solid. *Philos. Mag. A* **2000**, *80*, 2827–2840. [CrossRef]
22. Otero-de-la-Roza, A.; Luaña, V. Gibbs2: A new version of the quasi-harmonic model code. I. Robust treatment of the static data. *Comput. Phys. Commun.* **2011**, *182*, 1708–1720. [CrossRef]
23. Otero-de-la-Roza, A.; Abbasi-Pérez, D.; Luaña, V. Gibbs2: A new version of the quasiharmonic model code. II. Models for solid-state thermodynamics, features and implementation. *Comput. Phys. Commun.* **2011**, *182*, 2232–2248. [CrossRef]

24. Liu, Z.; Sun, X.; Zhang, C.; Hu, J.; Song, T.; Qi, J. Elastic Tensor and Thermodynamic Property of Magnesium Silicate Perovskite from First-principles Calculations. *Chin. J. Chem. Phys.* **2011**, *24*, 703–710. [CrossRef]
25. Carpenter, M.A.; Salje, E.K.H.; Howard, C.J. Magnetoelastic coupling and multiferroic ferroelastic/magnetic phase transitions in the perovskite $KMnF_3$. *Phys. Rev. B* **2012**, *85*, 224430. [CrossRef]
26. Zhong, W.; Vanderbilt, D.; Rabe, K.M. Phase Transitions in $BaTiO_3$ from First, Principles. *Phys. Rev. Lett.* **1994**, *73*, 1861–1864. [CrossRef]
27. King-Smith, R.D.; Vanderbilt, D. First-principles investigation of ferroelectricity in perovskite compounds. *Phys. Rev. B* **1994**, *49*, 5828–5844. [CrossRef]
28. Kohn, W.; Sham, L.J. Self-Consistent Equations Including Exchange and Correlation Effects. *Phys. Rev.* **1965**, *140*, A1133–A1138. [CrossRef]
29. Blaha, P.; Schwarz, K.; Madsen, G.K.H.; Kvasnicka, D.; Luitz, J. *WIEN2k: An Augmented Plane Wave and Local Orbitals Program for Calculating Crystal Properties*; Vienna University of Technology: Vienna, Austria, 2001.
30. Schwarz, K.; Blaha, P.; Trickey, S. Electronic structure of solids with WIEN2k. *Mol. Phys.* **2010**, *108*, 3147–3166. [CrossRef]
31. Singh, D.; Nordström, L. *Planewaves, Pseudopotentials and the LAPW Method*, 2nd ed.; Springer: New York, NY, USA, 2006.
32. Perdew, J.P.; Wang, Y. Accurate and simple analytic representation of the electron-gas correlation energy. *Phys. Rev. B* **1992**, *45*, 13244–13249. [CrossRef]
33. Perdew, J.P.; Burke, K.; Ernzerhof, M. Generalized Gradient Approximation Made Simple. *Phys. Rev. Lett.* **1996**, *77*, 3865. [CrossRef]
34. Perdew, J.P.; Burke, K.; Ernzerhof, M. Generalized Gradient Approximation Made Simple [Phys. Rev. Lett. 77, 3865 (1996)]. *Phys. Rev. Lett.* **1997**, *78*, 1396. [CrossRef]
35. Perdew, J.P.; Ruzsinszky, A.; Csonka, G.I.; Vydrov, O.A.; Scuseria, G.E.; Constantin, L.A.; Zhou, X.; Burke, K. Restoring the Density-Gradient Expansion for Exchange in Solids and Surfaces. *Phys. Rev. Lett.* **2008**, *100*, 136406. [CrossRef]
36. Wu, Z.; Cohen, R.E. More Accurate Generalized Gradient Approximation for Solids. *Phys. Rev. B* **2006**, *73*, 235116. [CrossRef]
37. Tran, F.; Laskowski, R.; Blaha, P.; Schwarz, K. Performance on molecules, surfaces, and solids of the Wu-Cohen GGA exchange-correlation energy functional. *Phys. Rev. B* **2007**, *75*, 115131. [CrossRef]
38. Tran, F.; Stelzl, J.; Blaha, P. Rungs 1 to 4 of DFT Jacob's ladder: Extensive test on the lattice constant, bulk modulus, and cohesive energy of solids. *J. Chem. Phys.* **2016**, *144*, 204120. [CrossRef] [PubMed]
39. Hidaka, M.; Ohama, N.; Okazaki, A.; Sakashita, H.; Yamakawa, S. A comment on the phase transitions in KMnF3. *Solid State Commun.* **1975**, *16*, 1121–1124. [CrossRef]
40. Karsai, F.; Tran, F.; Blaha, P. On the importance of local orbitals using second energy derivatives for d and f electrons. *Comput. Phys. Commun.* **2017**, *220*, 230–238. [CrossRef]
41. Charpin, T. *A Package for Calculating Elastic Tensors of Cubic Phase Using WIEN*; Laboratory of Geometrix: Paris, France, 2001.
42. Ivanov, Y.; Nimura, T.; Tanaka, K. Electron density and electrostatic potential of $KMnF_3$: A phase-transition study. *Acta Crystallogr. Sect. B* **2004**, *60*, 359–368. [CrossRef]
43. Hayatullah; Murtaza, G.; Khenata, R.; Muhammad, S.; Reshak, A.; Wong, K.M.; Omran, S.B.; Alahmed, Z. Structural, chemical bonding, electronic and magnetic properties of KMF3 (M = Mn, Fe, Co, Ni) compounds. *Comput. Mater. Sci.* **2014**, *85*, 402–408. [CrossRef]